Developing Correlation for Porosity and Permeability Between Mercury Intrusion and Gas Expansion Methods for Sandstone Core Plugs

Lucky Abiashue[1], *Yueping* Yu[1], *Omid* Mohammadzadeh[1], *Jules* Reed[2], *Lesley Anne* James[1]*

[1] Department of Process Engineering, Faculty of Engineering and Applied Science, Memorial University of Newfoundland St. John's, NL A1C 5S7, Canada.
[2] Premier Corex, UK

Abstract. This work contributes to generation of easy and accurate porosity and permeability data for sandstone core samples using mercury intrusion porosimetry (MIP) and gas expansion porosimetry and permeametry methods. Porosity and permeability obtained from MIP are often underestimated. MIP is faster and cheaper but its usage is warranted if the produced porosity and permeability data could be corrected based on a more accurate measurement method such as gas expansion. In this work, a correlation is developed between MIP and gas expansion porosity and permeability values by which MIP results could be corrected. MIP was used to estimate porosity and permeability from 19 trimmed core plug samples extracted from core drilled offshore Newfoundland and Labrador (Canada) with permeability range of 224 to 3,955.8 *mD* and porosity of 7.4 to 24.6%. The core plugs were used to measure the Klinkenberg-corrected permeabilities using steady-state flow of helium gas. The permeability was also calculated using several correlations including Heid, Jones-Owens, Sampath, and Florence, with the aid of Newton-Raphson iteration and graphical linear regression (MATLAB coding). In addition, a well-accepted correlation, known as Swanson model, was used to calculate core plug permeabilities from MIP data for comparison against measurements. Porosities of core plug samples were measured by helium pycnometry and then compared to measured values extracted from previous studies. The measured and calculated porosity and permeability results were compared between different methods, and their levels of variations were determined using statistical measures. This comparative analysis showed that the porosity values obtained using helium pycnometry are mostly greater than those obtained using MIP method, with an average difference of 9.8%. The permeability values obtained from Klinkenberg-corrected permeametry are greater than the results from MIP method with an average difference of 21.3%. The permeability data estimated using Swanson correlation exhibited higher error when compared to the Klinkenberg-corrected permeabilities, with an average percentage difference of 49.2%. Both porosity and permeability values from MIP are generally smaller than the values obtained from the more accurate gas porosimetry or permeametry methods. Developing Klinkenberg-corrected gas permeability plots can be challenging based on pressure ranges of interest; therefore, use of correlations to estimate gas permeability values is a common practice in routine core analysis. There is little or no study on these comparisons for sandstone samples in the literature. This work has the potential to form the basis of a guideline in generating Klinkenberg-corrected permeability for sandstone samples based on direct measurements as well as use of correlations.

1 Introduction

Data obtained from core analysis, including capillary pressure, permeability, and porosity is vital to assess and model reservoir-scale hydrocarbon flow. Hence, the accuracy of these data and the ease with which they are obtained are crucial. MIP method is a faster and cheaper method to analyze capillary pressure compared to centrifuge, porous plate, vapor desorption or coreflooding methods [1]. From the MIP test, very valuable rock properties are obtained such as porosity, injection pressure versus mercury saturation, and pore throat size distribution. The capillary pressure and pore throat size distribution can then be correlated to estimate the sample permeability. However, the MIP measurements are subject to some errors which make the data less accurate compared to other methods such as gas permeametry (for permeability measurement) or helium pycnometry (for porosity measurement). These errors arise from various sources such as sample size and shape, operating condition, mercury and penetrometer properties, core property measurement and conversion. The permeability results derived from the MIP method are estimated using a built-in correlation, and are generally lower than the Klinkenberg-corrected permeability data, obtained from gas permeametry [2]. Therefore, a correction needs to be developed to relate the permeability data obtained from these two methods. This is also the case when it comes to comparing porosity data from the MIP method to the values obtained from gas pycnometry. The porosity values from MIP method are generally smaller than those from gas pycnometry method [3]. Such a comparative study has not been done before yet in the literature.

* Corresponding author: ljames@mun.ca

The goal of this research is to find a correction correlation for permeability and porosity results obtained from the MIP method by comparing the results with permeability and porosity values obtained from more accurate methods (i.e., gas permeametry and helium pycnometry methods, respectively). The correction(s) can then be applied to future MIP measurements, resulting in better accuracy from a faster and cheaper porosity and permeability measurement method. The Klinkenberg-corrected permeability was also obtained using several correlations including Heid [15], Jones-Owens [16], Sampath [17], and Florence [18], with the aid of Newton-Raphson iteration and graphical linear regression (MATLAB coding). The correlation iteration results were then compared with the graphical linear regression results. In addition, a well-accepted correlation, known as Swanson model, was used to calculate core plug permeabilities from MIP data for comparison against measurements.

2 Mercury Intrusion Permeametry (MPI)

Using MIP, several rock properties are directly measured including porosity, pore size distribution and injection pressure versus saturation of mercury in the rock sample. The pore size distribution and mercury pressure vs. saturation information can then be used to calculate permeability of the rock sample. For instance, Katz and Thompson model [22] is used in 9500 Autopore IV Porosimeter for permeability calculation. In the MIP method, the mercury volume invading through a pore space is measured at incremental mercury injection pressures. A schematic diagram of intruded and extruded mercury volume as a function of applied pressure is illustrated in Figure 1. An important observation from this figure is the difference between the intruded and extruded mercury volume as a function of the applied pressure, as well as its maximum value at zero pressure (i.e., start of the saturation process and endpoint of the desaturation process) that exhibits mercury entrapment in the test sample. This signifies the destructive nature of the MIP test. When MIP was used for weak compressibility sandstone samples with permeability values greater than 1×10^{-15} μm^2, it was reported that the error in saturation data caused by the compression effect can be neglected [4]. The capillary pressure results obtained from the mercury intrusion capillary pressure (MICP) test are primarily useful in comparative studies of similar materials and determination of entry pressure for special core analysis (SCAL) [5]. A snapshot of the mercury porosimeter used in this study is shown in Figure 2.

3 Gas Permeameter

In a steady-state gas permeametry apparatus shown in Figure 3, when a gas phase passes through a confined permeable sample under steady state flow regime, the samples' permeability to gas can be calculated using Darcy's law according to Eq. 1:

$$k_g = \frac{2Q_1P_1\mu_g L}{A(P_1^2 - P_2^2)} \quad (1)$$

where P_1 is the test gas feed pressure (atm), P_2 is the sample's outlet gas pressure (atm), μ_g is gas viscosity (cP), L is the sample length (cm), A is the sample's crossflow sectional area (cm^2), and Q_1 is gas flow rate (L/s). Q_a and P_a measured under ambient pressure can also be used above the fractional line depending on measurement position.

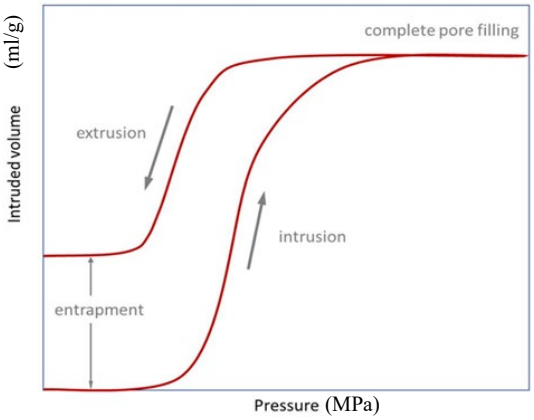

Fig. 1. Capillary pressure curves from the MICP test showing mercury entrapment in the test sample [13].

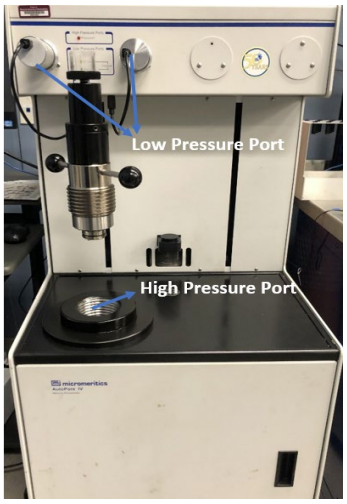

Fig. 2. A snapshot of 9500 Autopore IV Porosimeter

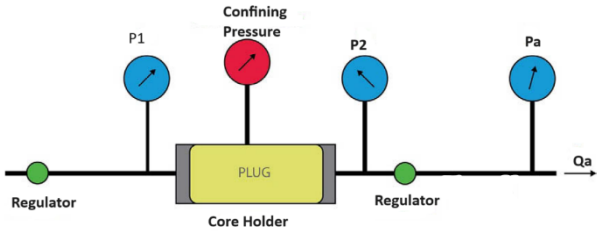

Fig. 3: Schematic diagram of a steady state gas permeameter [20]

Considering the gas slippage effect [19], the measured gas permeability values are generally bigger than the absolute permeability to a liquid, and Klinkenberg [6] discovered a linear correlation between sample's gas

permeability and inverse of the mean pressure across the test sample as shown in Eq. 2:

$$k_g = k_l[1 + \frac{b_k}{P_m}] \quad (2)$$

where k_l is equivalent absolute liquid permeability (mD), k_g is gas permeability (mD), P_m is the mean pressure across the sample (atm), and b_k is gas slippage factor (atm).

Eq. 2 represents a linear correlation between k_g and $\frac{1}{P_m}$ for each sample, where the slope is determined by $k_l b_k$, and it differs when various test gas types with different slippage factors and viscosity are used. Under lab testing conditions, usually between 3 to 5 measured pressure points are collected through which a linear correlation is regressed in order to estimate the equivalent liquid permeability, which is the interception of the linear extrapolation according to Eq. 2, when mean pressure approaches infinity (i.e., ultimate compression approximation of gas molecules to a liquid testing medium), (Figure 4).

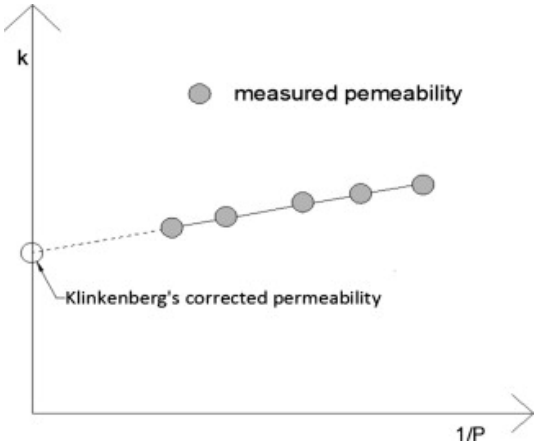

Fig. 4: Estimation of Klinkenberg corrected permeability using linear regression of measured gas permeability data [24]

4 Swanson Model

A correlation between effective pore throat diameter and air and brine permeabilities was developed by Swanson [8]. This correlation is generally used for permeability calculation when detailed pore structure data are available, similar to the information generated by the MICP method. The effect of sample size on the magnitude of capillary pressure (P_c) curve apex was also studied using MICP tests with core plugs as well as drill cuttings, and the impact was found insignificant [14]. The permeability-capillary pressure relationship was proposed in the following form:

$$k = a(S_b/P_c)^c_{max} \quad (3)$$

where k is permeability, a and c constants depend on the rock type (i.e., carbonate or sandstone) and fluid type (i.e., air or brine), respectively, and S_b is the percent bulk volume occupied by mercury.

Guo et al. improved the Swanson's model by introducing a parameter called "capillary parachor" which describes the rock pore structure, hence strongly depends on rocks permeability [8]. Figure 5 shows how to obtain Swanson parameter from capillary pressure data.

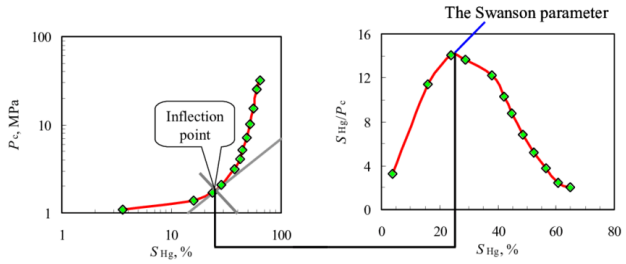

Fig. 5. Diagram showing how to obtain Swanson parameter and capillary parachor from MICP data [8]

5 Helium Porosimetry

Porosity is described as the ratio of pore volume to bulk volume in a given porous sample [9]. It expresses how porous the rock is; hence, it dictates the rock capacity for storing fluids. Porosity is mathematically defined as

$$\phi = V - \frac{Vs}{V} = \frac{Vp}{V} \quad (4)$$

where "volume of solids" is denoted by V_S, "total bulk volume" is denoted by V, and "pore volume" is given as $Vp = V - Vs$

The porosimeter uses the gas expansion technique governed by Boyle's law. This allows for the measurement of the pore volume, and hence for the calculation of porosity

6 Methodology

In this work, nineteen (19) core plugs extracted from a core drilled in offshore Newfoundland and Labrador (Canada) were analysed for permeability and porosity using air permeametry and MIP with 9500 Autopore IV Porosimeter, respectively. The core plug samples were extracted from a homogeneous full core, collected from 3955.50.40 – 4099.95 *m* depth interval. The MIP test was used for porosity measurement and permeability estimation. Some porosity measurements, using helium pycnometry, were done previously by Core Laboratories Inc. [23] on several core plugs from the same depth range as that of the samples used in this research work. For the comparison purposes, these pycnometry results were borrowed from a publicly available database. The depth information associated with these porosity values corresponds with the depths associated with the core plug samples tested in our research work. These porosity results, borrowed from the literature, were also validated by carrying out porosity measurement on 10 selected core plug samples in our lab using a Helium pycnometer.

6.1. Steady State Gas Permeametry

A single plug coreflooding setup was used to measure gas permeability, followed by Klinkenberg correction. The apparatus for steady state gas permeability measurement is

schematically shown in Figure 6. The shut-in valve and leak test valve were added to the conventional permeameter setup to allow testing for leakage, and a bypass valve was added in order to expedite saturating the test sample with gas. Normally, an adjustable valve is used as a back pressure regulator (BPR) in such gas permeametry measurements. However, it was realized that use of such adjustable valve as the BPR for testing high permeability samples (i.e., $k \geq 2000\ mD$) led to non-Darcy flow conditions; therefore for this subset of high-permeability core plugs, a standalone BPR with internal oscillating membrane was used.

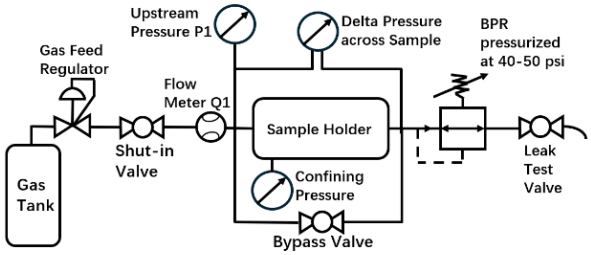

Fig. 6: Steady-state gas permeameter apparatus

Typically, 3 or 5 experimental flow rate and pressure points are extracted in such steady-state gas permeametry measurement that results in 3-point or 5-point Klinkenberg corrected permeability value; however, collecting these many experimental datapoints could be challenging and/or time consuming. Therefore, various correlations were developed with a smaller number of measured lab datapoints requirements in which use of Newton-Raphson iteration results in determination of Klinkenberg corrected permeability value. The Newton-Raphson iteration is designated to solve/obtain the interception point of the correlation function. A graphical representation of Newton-Raphson iteration method is provided in Figure 7 with the mathematical interpretation presented in Eq. 5:

$$x_{n+1} = x_n - \frac{f(x_n)}{f'(x_n)} \tag{5}$$

A stepwise procedure was developed and followed in this study using the customized steady state permeameter illustrated in Figure 6. This stepwise procedure is schematically presented in Figure 8. The recorded values in MS Excel, directly taken from lab experiments, were all exported to MATLAB environment where a coding scripts for Newton-Raphson iteration method was developed and executed. In this study, the lowest gas permeability datapoint under steady state flow regime near to the interception point was taken as the initial value (i.e., x_n in Eq. (5)) into the iteration process, and the iterations were run until the error became smaller than a pre-set threshold that resulted in obtaining the final iterated value as the "Klinkenberg corrected permeability" under each designated correlation. This loop iteration procedure is schematically shown in Figure 9.

In addition to the use of correlations, the Klinkenberg corrected permeability was also obtained using graphical linear regression method and was then compared with the permeability results from iterations using correlations. An example of graphical representation of Klinkenberg corrected permeability using linear regression with MATLAB coding script is provided in Figure 10.

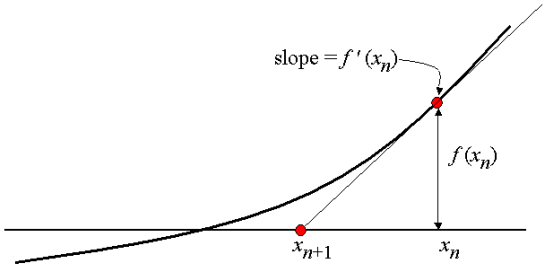

Fig. 7: Graphical representation of Newton-Raphson iteration method [21]

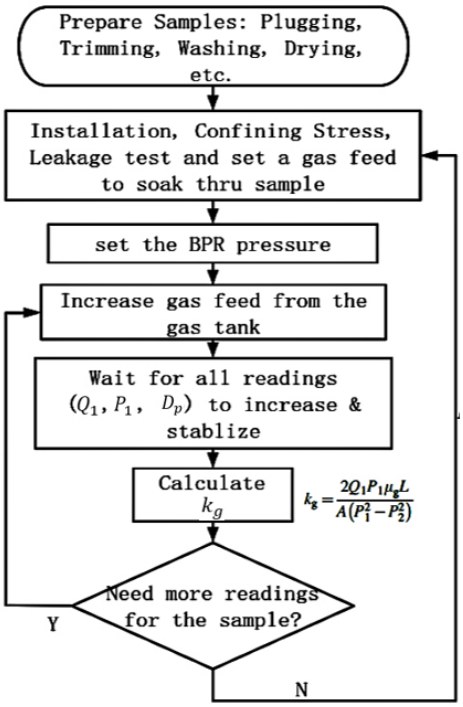

Fig. 8: The stepwise procedure followed in this study to measure gas permeability of a core plug

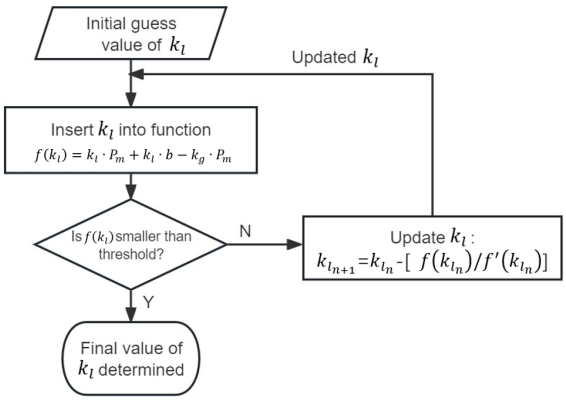

Fig. 9: Logical loop of Newton-Raphson iterations used in this study to calculate Klinkenberg corrected permeability using each correlation based on lab data

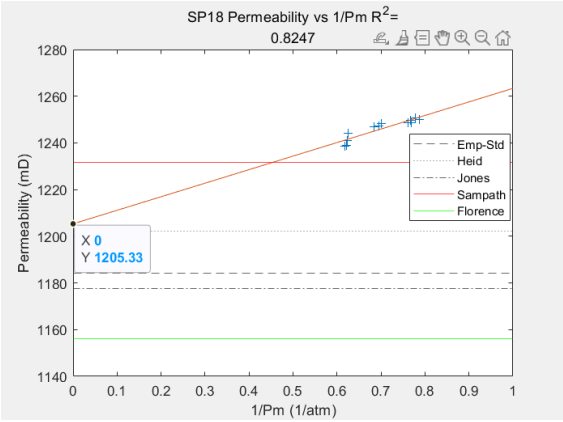

Fig. 10: Comparison between Klinkenberg corrected permeability obtained from linear regression and those obtained from Newton-Raphson iterations associated with correlations. The scattered datapoints are measured gas permeabilities. The y-intercept of solid dark red line passing through datapoints shows Klinkenberg corrected permeability from linear regression method. The height of each horizontal line represents the Klinkenberg corrected permeability using Newton-Raphson iterations associated with various correlations.

6.2. MIP

Micromeritics AutoPore IV 9500 equipment was used to measure porosity and pore size distribution of core plugs using pressurized mercury. This equipment has two low-pressure ports and one high-pressure port. Mercury is injected into the porous material at increasing pressures up to 33,000 *psig*. The intrusion volume is measured at each pressure, which corresponds to the volume of pores associated with various pore sizes occupied by mercury at that particular invasion pressure. This is a destructive testing method, and the sample must be disposed off properly after testing. This is the procedure we followed in this study to measure porosity using MIP test: some small rock fragments, taken from each core plug, are placed into a suitable penetrometer and then installed into the low-pressure chamber, evacuated, and backfilled with mercury. During the low-pressure mode measurement cycle, a gas pressure of up to 35.5 *psig* is used to displace the mercury in order to measure the volume of large pores. This is subsequently transitioned to implementing higher pressures, in the order of 33,000 *psig* using an oil hydraulic pressure chamber during the high-pressure measurement mode, to force the mercury into the very small pore spaces. As pores are filled, mercury moves out of the capillary stem. This stem is surrounded by a metal sleeve or sheath which together with the column of mercury constitutes a capacitor, which is in turn arranged in an electrical sensing circuit. The amount of mercury intruded into pores can then be quantified. After each pressurization event (pneumatic and hydraulic), the pressure is decreased, returning the system to ambient atmospheric pressure.

6.3. Helium Pycnometry

Detailed scope included generation of a calibration curve using some standard cylindrical steel samples of known pore volumes which were all tested using an inhouse designed and manufactured helium pycnometer. The principle of Boyle's Law was applied during calibration and testing of the setup. In this method, a calibration curve was generated by monitoring the equilibrium pressure of helium gas when expanded from the standard chamber (V_1 to V_2) to the sample chamber (V_2 to V_1) as seen in Figure 11. To prepare the calibration curve, 11 standard cylindrical steel samples of different known pore volumes were tested in the gas pycnometer at an overburden pressure of 400 ± 5 *psig* and initial pressure of 26.360 ± 0.01 *psig*. After generating the calibration curve, the core plug samples with unknown porosities were placed in the sample chamber, and the same procedure was carefully followed to determine the equilibrated pressure difference, based on which the pore volume was determined from the calibration curve. The sample bulk volume was determined using geometrical calculations. Having the physical dimensions of each core plug measured three times, the average values of bulk volumes were calculated from the dimensions. Porosity was calculated by dividing the pore volume by bulk volume.

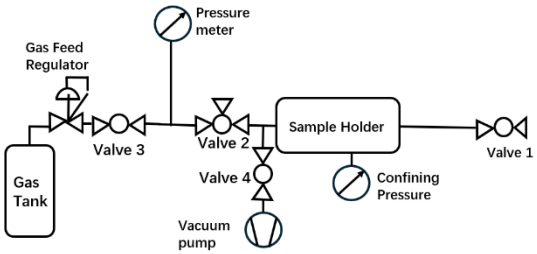

Fig. 11: Schematic diagram of in-house built helium pycnometer

6.4. Permeability Calculation using Swanson Model

The Swanson model presented in Eq. (3) was used in this study in order to estimate permeability from the MIP data where k is permeability (mD), S_b is mercury saturation (mg/g), and P_c is mercury injection pressure (MPa). Considering the wetting phase and sample lithology in this study (i.e., air and sandstone, respectively), the constants a and c in Eq (3) are 399 and 1.691, respectively. The Swanson parameter $(S_b/P_c)_{max}$ is the apex of the S_b/P_c (i.e., ratio of mercury saturation to pressure) against S_b in % (i.e., percentage volume of pore space occupied by mercury) [10, 8].

7 Results and Discussions

7.1. Klinkenberg Corrected Gas Permeability

Nineteen core plug samples were tested for gas permeability, and the results were processed using graphical linear regression analysis with MATLAB coding script as well as original Klinkenberg correlation (Table 1).

7.2. Permeability Estimation Using Correlations Based on Gas Permeametry Data

In addition to Klinkenberg-based correction method for gas permeametry data, four other correlations including Heid, Jones-Owens, Sampath, and Florence correlations were used in order to estimate the permeability. Note that these four correlations employ Newton Raphson iteration procedure discussed in section 6.1 with the same raw gas permeability data collected for Klinkenberg correction

calculations. The results are listed in Table 1. To determine the percentage variation of different correlations, we assume that the permeability values corrected using graphical linear regression method, based on Klinkenberg theory, are the most accurate values. To explain the % difference and accuracy of predictions using these iterative correlation calculations, it is important to consider the ranges of properties based on which each of these four correlations were originally developed (Table 2).

Assuming graphical linear regression Klinkenberg estimation to be the most accurate permeability determination method, the gas permeability values obtained using other correlations were compared against this permeability estimation procedure, with the average percentage difference and maximum percentage difference parameters calculated (Table 3) for comparisons against the more accurate permeability values. These statistical assessments, combined with the specific application parameter range(s) and rock typing information associated with developing each correlation suggests a more elaborate view of which correlation provides more accurate permeability predictions and why. According to this information, Jones-Owens correlation provided the most accurate permeability estimations, according to the average absolute value of offset percentage for sandstone samples tested in this study. However, Sampath correlation, which was developed based on the information extracted from tight gas sandstone samples from Cotton Valley, provided the least accurate, but the highest, permeability values for the core plug samples tested in this study.

7.3. Permeability Estimation using MIP Method

Using built-in correlation in mercury porosimeter (i.e., Katz and Thompson model [22]), permeabilities of the samples were estimated using information obtained during MIP. The estimated permeability values are listed in Table 4.

7.4. Permeability Estimation Using Modified Swanson Model

With the information obtained during MIP measurements, another correlation, known as Swanson model discussed in section 4, was used in order to calculate permeabilities. The results are listed in Table 5.

7.5. Comparison of Different Permeability Results

In this study, two sources of measurements were used for permeability determination: a) raw data from gas permeametry tests, which were then processed using Klinkenberg standard correlation, graphical linear regression algorithm proposed by Klinkenberg, and also four other correlations namely Heid, Jones-Owens, Sampath, and Florence; and b) raw data from MIP, which were then processed for permeability calculation using Katz and Thompson model [22] as well as modified Swanson model [8]. Among gas permeametry data, the values obtained using Klinkenberg's linear regression algorithm were taken as the most accurate values, hence were used in comparisons with permeability estimations using MIP data (Table 6, Figure 12). As seen in the histogram presented in Figure 12, the permeability values estimated using Katz and Thompson model [22] are closer to corrected gas permeability values, but there is significant difference between the permeability data estimated using modified Swanson model when compared to the reference corrected gas permeametry values. The ranges of variation for permeability values obtained from modified Swanson model [8] as well as Katz and Thompson model [22] are 84.7–2140.0 *mD* and 154.3 – 3953.6 *mD*, respectively, while the direct permeability measurement using gas permeametry resulted in permeability values in the range of 200.1 – 3955.6 *mD.* The permeability values obtained from the MIP data using Katz and Thompson model [22] seem to be more accurate than the ones obtained based on the MIP tests but with the application of modified Swanson model [8] (refer to last two columns of Table 6 that contain the % relative difference values with respect to the reference corrected gas permeability data). This is also in line with the observations documented in the literature [11].

In Figures 13 and 14, the calculated permeability values using Katz and Thompson model [22] as well as modified Swanson model [8], based on the MIP tests, are plotted versus equivalent liquid permeability, obtained from gas permeametry measurements. Note that the corrected permeability values from gas permeametry tests were obtained using Klinkenberg's linear regression algorithm. These parity plots will help understand the representativeness of any of these two models for permeability estimation (based on MIP method) when compared to a direct permeability measurement method, and also provide some clarity on whether a correlation could be found in order to correct the estimated permeability values based on comparison against a more accurate direct measurement method. The red dotted lines show the $x=y$ baseline, and the blue dotted lines represent the linear trendlines fitted to the data points. The scatter error associated with these parity plots is visually determined by how the data points spread around the diagonal x=y baseline. Clearly, estimating permeability based on the MIP data has some error when compared to direct gas permeametry; however, the permeability values estimated using built-in correlation associated with the MIP equipment (i.e., Katz and Thompson model [22]) were closer to direct measurements when compared to other employed model that also uses the MIP data (i.e., modified Swanson model [8]). The built-in Katz and Thompson model [22] in the mercury porosimeter almost always underestimated the permeability values (except only two datapoints for samples SP3 and SP14). The linear correlation obtained between the Klinkenberg-corrected permeability values and the estimated ones using Katz and Thompson [22] model could be safely used to convert the mercury intrusion permeability estimation to equivalent liquid permeability, considering a slight room for error as depicted in Figure 13 from the coefficient of determination value. However for the permeability values estimated using the modified Swanson model [8], there is no consistency when it comes to comparison against the direct measurement method, which is evident from the weak linear trend and low coefficient of determination in Figure 14.

Table 1. Klinkenberg corrected gas permeability using graphical linear regression and Klinkenberg original correlation, along with the ones predicted using Heid, Jones-Owens, Sampath, and Florence correlations with the aid of Newton Raphson iteration – raw gas permeability data were processed using MATLAB script.

Sample No	Depth (*m*)	Klinkenberg corrected *k* (*mD*) using graphical linear regression estimation	Klinkenberg corrected *k* (*mD*) using Klinkenberg original correlation	*k* (*mD*) using Heid correlation	*k* (*mD*) using Jones-Owens correlation	*k* (*mD*) using Sampath correlation	*k* (*mD*) using Florence correlation	Correlation closest to graphical linear regression
SP01	3959.40 - 3959.79	984.2	982.4	990.4	965.8	1021.1	942.7	Klinkenberg
SP03	3961.85 - 3962.32	465.1	470.7	470.8	457.5	488.7	433.7	Klinkenberg
SP04	3967.28 -39 67.98	1,821.7	1929.9	1953.1	1912.1	2004.0	1934.2	Jones
SP05	3970.33 - 3970.67	3,205.6	3175.0	3214.3	3159.1	3272.6	3132.6	Heid
SP06	3970.96 - 3971.20	2,474.7	2456.1	2490.5	2445.3	2540.1	2419.5	Heid
SP07	3973.29 - 3973.58	2,203.7	2179.1	2206.8	2162.9	2255.4	2133.1	Heid
SP08	3978.57 - 3979.29	859.3	857.8	863.1	840.7	891.3	814.1	Klinkenberg
SP10	4009.40 - 4009.60	212.5	238.3	234.1	226.1	246.8	211.2	Florence
SP13	4017.54 - 4017.80	385.9	426.9	423.9	410.3	442.0	380.7	Florence
SP14	4020.98 - 4021.28	241.0	248.1	243.8	235.4	256.7	216.9	Heid
SP17	4027.94 - 4028.17	200.1	244.2	240.5	232.4	253.6	222.5	Florence
SP18	4035.83 - 4036.08	1145.3	1140.4	1152.4	1125.7	1185.0	1101.2	Klinkenberg
SP19	4037.15 - 4037.49	791.6	809.7	814.4	793.1	841.4	767.5	Jones
SP20	4040.31 - 4040.52	1395.3	1415.0	1430.3	1397.6	1469.1	1374.0	Jones
SP22	4043.20 - 4043.39	2170.7	2153.6	2180.9	2137.3	2229.9	2114.6	Heid
SP23	4045.73 - 4046.05	3012.4	3022.5	3054.0	2995.7	3116.5	2967.3	Klinkenberg
SP30	4082.12 - 4082.34	1128.6	1200.7	1219.8	1195.7	1249.0	1178.4	Florence
SP31	4083.86 - 4084.10	3955.6	3884.0	3914.6	3843.5	3988.9	3820.1	Sampath
SP32	4088.01 - 4088.37	1854.4	1997.3	2019.8	1976.7	2068.7	1949.8	Florence

Table 2. Range of parameters and rock type(s) based on which correlations were developed for permeability estimation using gas permeability raw data.

Correlation	Equation	Rock type for which the correlation was developed	Permeability range (*mD*)
Heid	$b_k = 11.419(k_\infty)^{-0.39}$	Artificial sandstones	10^{-1} to 10^{4}
Jones-Owens	$b_k = 12.639(k_\infty)^{-0.33}$	Tight gas sandstones	10^{-3} to 10^{1}
Sampath	$b_k = 13.851\left[\frac{k_\infty}{\emptyset}\right]^{-0.53}$	Tight gas sandstones	10^{-2} to 10^{2}
Florence	$b_k = \beta[\frac{k_\infty}{\emptyset}]^{-0.5}$	Tight gas sandstones	10^{-5} to 10^{0}
Standard Klinkenberg	$k_g = k_\infty[1 + \frac{b_k}{P_m}]$	Sandstone	10^{1} to 10^{3}
b_k: Gas slippage factor; $\emptyset$: porosity; k_∞ and k_l are equivalent liquid permeability from gas permeametry tests.			

Table 3. Statistical comparison of permeability estimations using various correlations compared to linear regression Klinkenberg correction (graphical method).

Correlation	Ave. absolute % difference with respect to linear regression *k* estimates	Ave. % difference with respect to linear regression k estimates	Biggest % difference compared to linear regression *k* estimates
Heid	4.1%	3.99%	10.19% Lowest
Jones-Owens	3.47% Lowest	1.45%	16.16%
Sampath	7.26% Highest	7.26% Highest	26.73% Highest
Florence	4.14%	-1.31% Lowest	11.2%
Klinkenberg Standard	4.17%	3.52%	12.14%

Table 4. Permeability estimation using MIP data based on Katz and Thompson correlation [22].

Sample	*k* calculated using MIP data based on Katz and Thompson model (*mD*)
SP01	652.0
SP03	658.2
SP04	1747.4
SP05	2451.2
SP06	1704.5
SP07	2072.5
SP08	495.1
SP10	181.2
SP13	353.9
SP14	359.2
SP17	154.3
SP18	753.9
SP19	618.7
SP20	1207.5
SP22	1212.2
SP23	2867.7
SP30	605.1
SP31	3953.6
SP32	1669.1

Table 5. Samples permeability calculated from Swanson model [8]

Sample	$(H_g/P_c)_{max}$	*k* calculated using Swanson model (*mD*)
SP01	1.20	543.1
SP03	1.50	792.0
SP04	2.01	1299.2
SP05	2.30	1631.8
SP06	1.90	1181.3
SP07	2.20	1513.6
SP08	0.50	123.6
SP10	0.59	163.5
SP13	0.79	267.8
SP14	0.67	202.7
SP17	0.40	84.7
SP18	1.17	520.3
SP19	1.09	461.6
SP20	1.21	550.8
SP22	1.20	543.1
SP23	1.20	543.1
SP30	0.90	333.9
SP31	2.70	2140.0
SP32	1.90	1181.3

Table 6. Comparison of permeability values obtained from different methods.

Sample No	Depth (m)	*k* (*mD*)			Relative Difference (%)	
		Modified Swanson Model [8]	Katz and Thompson Model [22]	Gas Permeametry	$(k_{L,eq}- k_{Katz\ \&\ Thompson})/ k_{L,eq})\times100$	$(k_{L,eq}- k_{Swanson})/ k_{L,eq})\times100$
SP01	3959.40 - 3959.79	543.1	652.0	984.2	33.8	44.8
SP03	3961.85 - 3962.32	792.0	658.2	465.1	-41.5	-70.3
SP04	3967.28 -39 67.98	1299.2	1747.4	1821.7	4.1	28.7
SP05	3970.33 - 3970.67	1631.8	2451.2	3205.6	23.5	49.1
SP06	3970.96 - 3971.20	1181.3	1704.5	2474.7	31.1	52.3
SP07	3973.29 - 3973.58	1513.6	2072.5	2203.7	6.0	31.3
SP8	3978.57 - 3979.29	123.6	495.1	859.3	42.4	85.6
SP10	4009.40 - 4009.60	163.5	181.2	212.5	14.7	23.1
SP13	4017.54 - 4017.80	267.8	353.9	385.9	8.3	30.6
SP14	4020.98 - 4021.28	202.7	359.2	241.0	-49.0	15.9
SP17	4027.94 - 4028.17	84.7	154.3	200.1	22.9	57.7
SP18	4035.83 - 4036.08	520.3	753.9	1145.3	34.2	54.6
SP19	4037.15 - 4037.49	461.6	618.7	791.6	21.8	41.7
SP20	4040.31 - 4040.52	550.8	1207.5	1395.3	13.5	60.5
SP22	4043.20 - 4043.39	543.1	1212.2	2170.7	44.2	75.0
SP23	4045.73 - 4046.05	543.1	2867.7	3012.4	4.8	82.0
SP30	4082.12 - 4082.34	333.9	605.1	1128.6	46.4	70.4
SP31	4083.86 - 4084.10	2140.0	3953.6	3955.6	0.1	45.9
SP32	4088.01 - 4088.37	1181.3	1669.1	1854.4	10.0	36.3

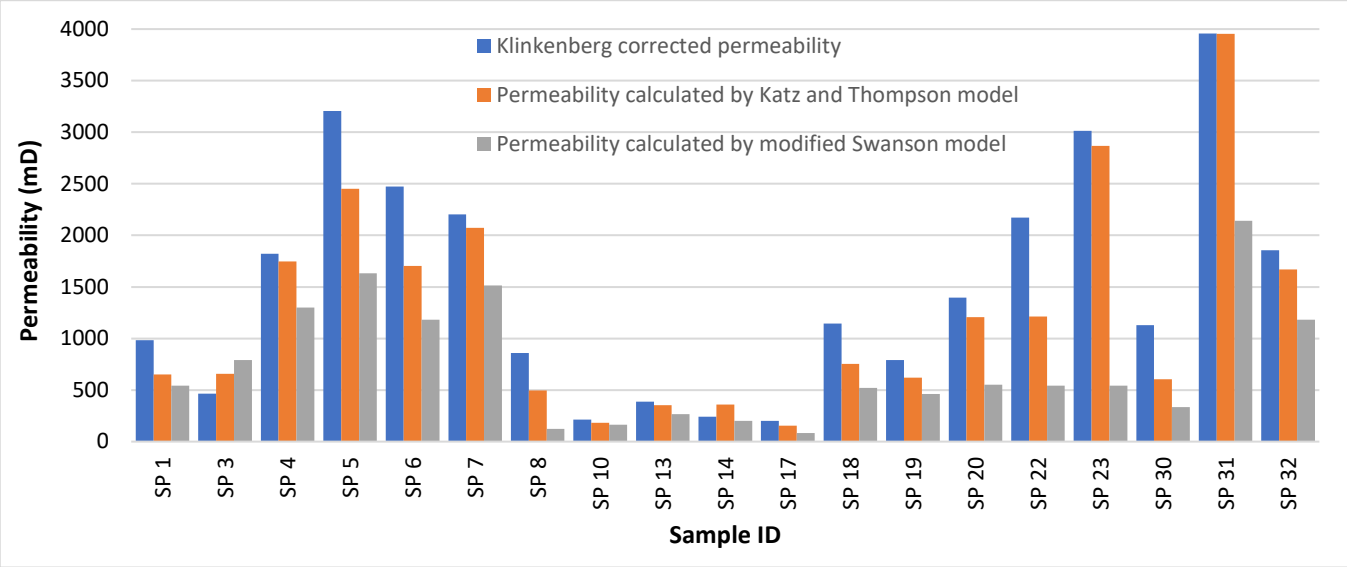

Fig. 12. Comparison between permeability values from MIP data using Katz and Thompson model [22], predicted values from modified Swanson model [8], and the reference gas permeability values from Klinkenberg's linear regression algorithm.

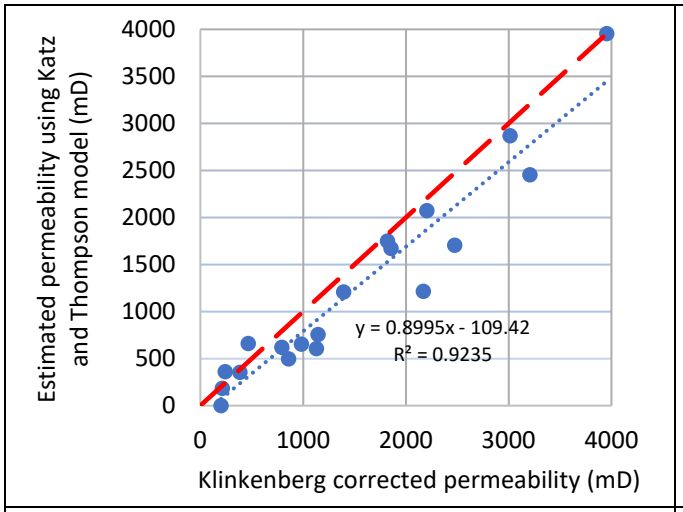

Fig. 13. Correlation between permeability values from MIP data (Katz and Thompson model [22]) and reference values from Klinkenberg's linear regression algorithm.

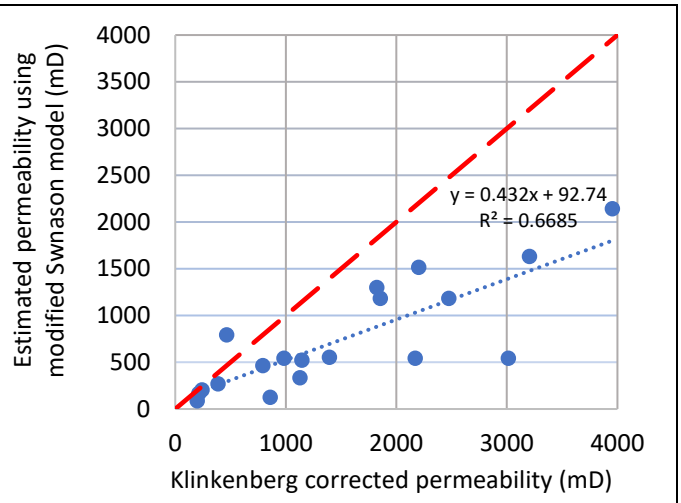

Fig. 14. Correlation between permeability values from MIP data (modified Swanson model [8]) and reference values from Klinkenberg's linear regression algorithm.

7.6. Comparison of Different Porosity Results

Porosity of the tested samples in this study come from MIP and helium pycnometry. For most of the samples tested in this study, helium pycnometry method provides greater porosity values than those obtained from the MIP method. This is in agreement with observations from the literature [12]. The porosity values obtained from the helium pycnometry range from 7.4% to 24.6% while those measured with mercury intrusion range from 11.4% to 22.0%. These samples all have high porosity values, which is in agreement with their sandstone lithology. In Figure 16, the porosity values from helium pycnometry are plotted versus those from the MIP test. There is a weak correlation between the porosity values from these two methods, and the data spread around the red dotted line of $x=y$ shows the scatter error associated with the porosity measurement. There are two samples in this plot, highlighted with orange data marker colour, that do not agree with the trend observed for the rest of the datapoints, and act as outliers that deteriorate the accuracy of linear trendline fitted to the data. The comparison of the porosities from the two methods are visualised in the histogram presented in Figure 15. We assume the helium pycnometry method to be a more accurate and representative porosity measurement method compared to the MIP method because of the representativeness of tested sample (i.e., whole sample for helium pycnometry versus a small cutout in MIP), non-destructive nature of gas vs. mercury in damaging the pore structure, and the ease/possibility of measurement repeat on the same sample (not possible for MIP). Therefore, it is attempted to see how close the MIP measurements could be to the more accurate and representative helium pycnometry data (Table 7, Figures 15 and 16). Although most of the results from both methods were close to each other but few samples had higher deviations such the SP04 and SP13 (i.e., orange datapoints in Figure 16). This resulted in a low R^2 value. However, if we do not consider these two datapoints in the linear trend fitting, a much better correlation could be obtained. Considering the overall

agreement between the majority of the samples, this correlation can be useful in adjusting the MIP porosity values to get closer to the helium pycnometry equivalents.

8 Conclusions

Depending on the level of accuracy needed for the test, the permeability and porosity results from 9500 Autpore IV Porosimeter can be useful while considering the level of deviation from values obtained by other methods. The porosity and permeability results from the MIP test can be improved by applying the correction correlations proposed in this study to obtain more accurate results, comparable to the data obtained using more reliable measurement methods. This research work proposes correction correlations to modify data acquired from 9500 Autpore IV Porosimeter. Through this correction effort, more representative porosity and permeability values will be obtained based on MIP method. The proposed correction correlations are only applicable to sandstone samples; therefore, future research could be focused on developing the same for other rock types. In addition, more accurate MIP measurements could be done by selecting more representative rock samples, preferably the full diameter thin sections with the aid of proper penetrometer sizes. Other limitation is the unavailability of the total samples to directly measure the porosity instead of using data from the literature. In addition, having more samples could generate a more statistically representative correlation(s). This research could be improved on by carrying out both the porosity and permeability measurement tests on the same sample. This can be done by first carrying out the gas permeametry and pycnometry tests before using the same sample for MIP using a larger penetrometer. This will likely reduce some errors.

When it comes to comparing the Klinkenberg permeability models, Jones-Owens correlation provides the most accurate predictions when compared against the graphical approach of linear regression whereas Sampath and Florence correlations provide overestimated and underestimated predictions, respectively, compared to the graphical approach developed using direct gas permeametry measurements. Deviations between direct permeability measurements and predictions using correlations are attributed to the differences in permeability ranges for samples used in developing these correlations with those associated with the core plug samples we used in this study. For instance, the Florence correlation was developed from tight sandstone cores from Cotton Valley with permeability from 10^{-5} to 10 *mD*. The range of data for the Florence permeabilities are much smaller than the permeability range used in our study, proving that correlations should be used with caution outside the range of data based on which they were developed.

This project was supported by the Faculty of Engineering and Applied Science, Memorial University. We would like to thank Hibernia Management and Development Company (HMDC), Chevron Canada Ltd. And Mitacs for financial support.

References

1. N. I. Al-Bulushi, G. Kraishan, G. Hursan, PC *EAGE Conference* (2019).

2. M. Saki, S. Siahpoush, A.R. Khaz'ali, *Petrol Explor Prod Technol,* **10**, 2637–2644 (2020).

3. M. Mastalerz, A. Schimmelmann, A. Drobniak, Y. Chen, *AAPG Bulletin*, **97** (10):1621-1643 (2013).

4. J. Shafer, J. Neasham, *Society of Core Analysts* (2020).

5. A.J. Adams, PhD Thesis, Texas A&M University, pp 72-74 (2005).

6. L. Klinkenberg, *Drilling and Production Practice; American Petroleum Institute*, Washington, DC, USA (1941).

7. S.A. Farzaneh, M. Sohrabi, T. Solling, *Energy Fuels*, **35**, 5594-5612 (2021).

8. B. Swanson, *Journal of Petroleum Technology*, 33, **12**, 2488-2504 (1981).

9. L. Liu, H. Li, H. Zhou, S. Lin, S. Li, *Chinese Academy of Sciences*, China (2022).

10. S. Babak, D.W. Ruth, D. Green, V. Dragan, *International Symposium of the Society of Core Analysts* held in Avignon, France (2014).

11. D. Rasoul, E. Einar, J.D. Richard, *E3S Web of Conferences,* **89**, 01001 (2019).

12. M. Mastalerz, A. Schimmelmann, A. Drobniak, Y. Chen, *AAPG Bulletin*, **97** (10): 1621-1643 (2013).

13. Anton Parr. (n.d) Mercury Intrusion Porosimetry Basics: Measuring Pores in Solid, https://wiki.anton-paar.com/en/mercury-intrusion-porosimetry-basics-measuring-pores-in-solids/.

14. S. Apisaksirikul and T.A. Blasingame, *Unconventional Resources Technology Conference*, URTeC: 2460639, San Antonio, TX, USA, (2016).

15. J.G. Heid, J.J. McMahon, R.F. Nielsen, S.T. Yuster, *Drilling and production practice* (1950).

16. S.C. Jones, *SPE Annual Technical Conference and Exhibition* (1987).

17. K. Sampath, C.W. Keighin, *Journal of Petroleum Technology*, **34** (11), 2715-2720 (1982).

18. F.A. Florence, J.A. Rushing, K.E. Newsham, T.A. Blasingame, *Rocky Mountain Oil & Gas Technology Symposium*, (2007).

19. A. Kundt, E. Warburg, Ueber reibung und wärmeleitung verdünnter gase. Annalen der Physik, **232** (10), 177-211 (1875).

20. C. McPhee, J. Reed, I. Zubizarreta, *Elsevier Science,* (2015).

21. Brilliant.org wiki page, available at https://brilliant.org/wiki/newton-raphson-method/

22. A.J. Katz, A.H. Thompson, *Journal of Geophysical Research*, **B1**, pp. 599-607 (1987).

23. Core Laboratories, HMDC B16-17 Core Analysis Result, *CNLOPB Offshore Petroleum Board Data*

Information Hub, hibernia-b-16-17 | C-NLOPB Online Portal (arcgis.com), Accessed date: 12-06-2021. (1999).

24. G. Wang, T. Ren, K. Wang, A. Zhou, *Fuel*, **128**, 53-61 (2014).

Table 7. Core plug porosities from different methods,

Sample ID	**Depth (m)**	**Porosity from helium pycnometry [Core Laboratories, 1999]**	**Porosity from MIP (%)**	**Relative difference (%)** $\left[\frac{\varphi_{Helium\ Pycnometry} - \varphi_{MIP}}{\varphi_{Helium\ Pycnometry}}) \times 100\right]$
SP01	3959.40 - 3959.79	18.8	19.2	-2.1
SP03	3961.85 - 3962.32	21.6	20.6	4.6
SP04	3967.28 -3967.98	7.4	22.0	-197.3
SP05	3970.33 - 3970.67	22.0	19.0	13.6
SP06	3970.96 - 3971.20	21.3	20.3	4.7
SP07	3973.29 - 3973.58	21.9	20.5	6.4
SP08	3978.57 - 3979.29	20.5	17.9	12.7
SP10	4009.40 - 4009.60	16.1	14.3	11.2
SP13	4017.54 - 4017.80	24.6	18.3	25.6
SP14	4020.98 - 4021.28	19.1	17.6	7.9
SP17	4027.94 - 4028.17	12.2	11.4	6.6
SP18	4035.83 - 4036.08	19.7	18.1	8.1
SP19	4037.15 - 4037.49	20.2	17.9	11.4
SP20	4040.31 - 4040.52	19.0	17.9	5.8
SP22	4043.20 - 4043.39	19.5	18.0	7.7
SP23	4045.73 - 4046.05	21.6	20	7.4
SP30	4082.12 - 4082.34	17.9	15.7	12.3
SP31	4083.86 - 4084.10	21	18.8	10.5
SP32	4088.01 - 4088.37	20.3	20.5	-1.0

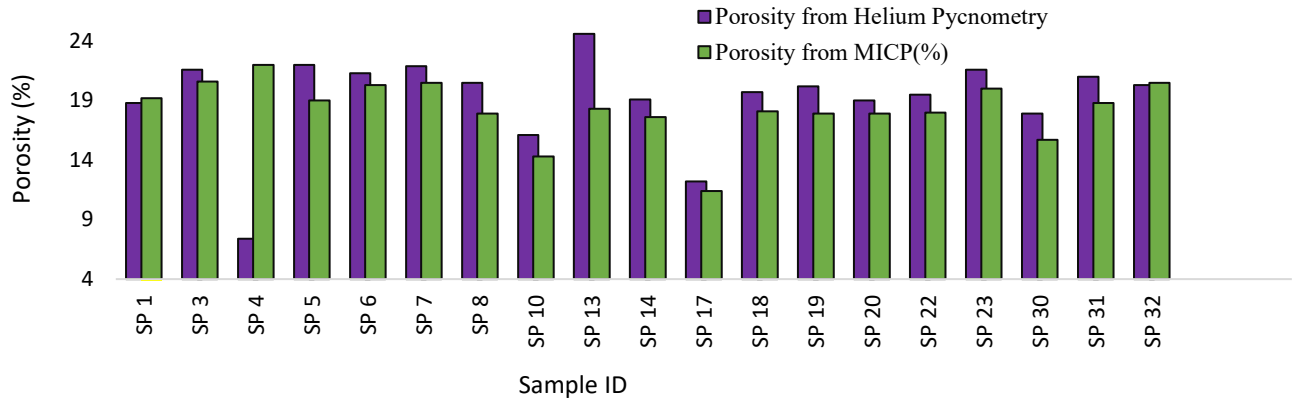

Fig. 15. Comparison of porosity values from helium pycnometry and MIP.

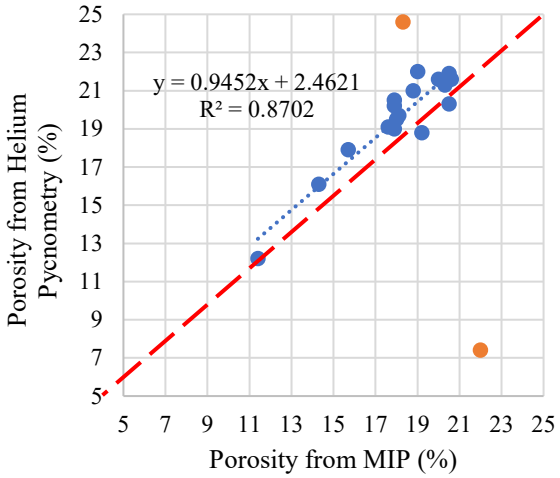

Fig. 16. Parity plot of porosity values measured using helium pycnometry vs. those from MIP.